Chaos and the continuum limit in the gravitational *N*-body problem: Integrable potentials

Henry E. Kandrup*
Department of Astronomy, Department of Physics, and Institute for Fundamental Theory, University of Florida, Gainesville, Florida 32611

Ioannis V. Sideris†
Department of Astronomy, University of Florida, Gainesville, Florida 32611

(Received 26 March 2001; revised manuscript received 19 June 2001; published 18 October 2001)

This paper summarizes a numerical investigation of the statistical properties of orbits evolved in ''frozen,'' time-independent *N*-body realizations of smooth, time-independent density distributions corresponding to integrable potentials, allowing for $10^{2.5} \leqslant N \leqslant 10^{5.5}$. Two principal conclusions were reached: (1) In agreement with recent work by Valluri and Merritt, one finds that, in the limit of a nearly ''unsoftened'' two-body kernel, i.e., $V(r) \propto (r^2+\epsilon^2)^{-1/2}$ for $\epsilon \to 0$, the value of the largest Lyapunov exponent χ does *not* decrease systematically with increasing *N*, so that, viewed in terms of the sensitivity of individual orbits to small changes in initial conditions, there is no sense in which chaos ''turns off'' for large *N*. However, it is clear that, for any finite ϵ, χ *will* tend to zero for sufficiently large *N*. (2) Even though χ does not decrease for an unsoftened kernel, there is a clear, quantifiable sense in which, as *N* increases, chaotic orbits in the frozen-*N* systems remain ''close to'' integrable characteristics in the smooth potential for progressively longer times. When viewed in configuration or velocity space, or as probed by collisionless invariants like angular momentum, frozen-*N* orbits typically diverge from smooth potential characteristics as a *power law* in time, rather than exponentially, on a time scale $\propto N^p t_D$, with $p \approx 1/2$ and t_D a characteristic dynamical, or crossing, time. For the case of angular momentum, the divergence is well approximated by a $t^{1/2}$ dependence, so that, when viewed in terms of collisionless invariants, discreteness effects act as a diffusion process that, presumably, can be modeled by nearly white Gaussian noise in the context of a Langevin or Fokker-Planck description. For position and velocity, the divergence is more rapid, characterized by a nearly linear power-law growth, t^q with $q \approx 1$, a result that likely reflects the effects of linear phase mixing. The inference that, pointwise, individual *N*-body orbits can be reasonably approximated by orbits in a smooth potential only for times $< N^{1/2} t_D$ has potential implications for various resonance phenomena that can act in real self-gravitating systems.

DOI: 10.1103/PhysRevE.64.056209 PACS number(s): 05.45.−a, 05.60.−k, 51.10.+y, 05.40.−a

I. INTRODUCTION AND MOTIVATION

Many astronomical objects, including, e.g., globular clusters, are typically modeled by bulk gravitational potentials that manifest a high degree of symmetry and that, being integrable, lead to completely regular characteristics with no possibility of chaotic behavior. One knows, however, that such bulk potentials constitute idealizations, the true system corresponding (at least approximately) to a realization of the gravitational *N*-body problem. The important point, then, is that motion in the *N*-body problem, even for an *N*-body system that samples a smooth, time-independent phase-space distribution corresponding to an integrable potential, is typically chaotic in the sense that orbits exhibit exponential sensitivity towards small changes in initial conditions [1]. This perhaps is not surprising. The true potential associated with a collection of point masses no longer possesses the symmetries of the original integrable potential, so that there is no reason why the orbits should not be chaotic.

However, what *is*, perhaps, surprising is the expectation, derived both from theoretical arguments [2,3] and from numerical simulations [4], that the *N*-body problem remains chaotic even for very large *N*. Suppose, e.g., that a system of total mass $M=1$ is represented by a collection of *N* points of mass $m=1/N$, so distributed as to sample the density distribution corresponding to an integrable potential. The claim then is that, when expressed in units of a natural dynamical, or crossing, time $t_D \sim 1/\sqrt{G\rho}$, with ρ a typical density, the characteristic time scale τ on which an initial perturbation in any given orbit tends to grow will not diverge for $N \to \infty$. In this sense, the degree of chaos manifested by individual orbits is not expected to ''turn off'' for very large *N*. There is an apparent consensus, motivated both from theory and numerical experiments, that τ should not increase without bound for $N \to \infty$, although there is some disagreement in the literature as to whether $\tau(N)$ should converge towards an *N*-independent value [2] or whether τ should instead slowly *decrease* with increasing *N* [3].

If, however, this be true, one is confronted with subtle questions of principle regarding the nature of the continuum limit. It is generally assumed [5] that, for sufficiently large *N*, a self-gravitating system of discrete point masses may be characterized adequately by a smooth phase-space density that solves the collisionless Boltzmann equation (CBE), i.e., the gravitational analogue of the Vlasov equation from plasma physics. The obvious point, then, is that time-independent solutions to this equation that manifest a high degree of symmetry correspond typically to bulk potentials

*Electronic address: kandrup@astro.ufl.edu
†Electronic address: sideris@astro.ufl.edu

that are integrable or, even if they be nonintegrable, admit large measures of regular orbits. But how is one to reconcile integrable or near-integrable behavior in such bulk potentials with the presumed fact that, even for very large N, individual orbits in the true N-body problem typically manifest chaotic behavior on a time scale $\sim t_D$?

Strictly speaking, there is no logical contradiction: It is completely possible for collective properties of an N-body system to be described correctly by the CBE, even if the characteristics associated with the self-consistent potential do not coincide, even approximately, with real N-body trajectories [6]. However, it *would* seem important to pin down carefully what is actually going on:

Is it really true that individual trajectories in the N-body problem are chaotic for very large N, even if the bulk potential associated with the system is integrable? The indications are that the answer to this is: yes. However, most of the work done to date on chaos in the N-body problem has focused on systems with comparatively small N and/or a hierarchy of masses, or, for larger systems, on comparatively short-time behavior. Little if any work has been done to provide estimates of honest Lyapunov exponents over intervals $\gg t_D$ for large N systems comprised of bodies of comparable mass.

How quickly do N-body trajectories diverge from smooth potential characteristics with the same initial condition, and is this divergence exponential or power law in time? Even presuming that the N-body problem is chaotic on a time scale $\sim t_D$, is there some time scale $T \gg t_D$ over which individual N-body trajectories are well approximated in a pointwise sense by characteristics given by the CBE?

These conceptual issues are also related directly to the problem of ''softening.'' It is generally recognized that, for small N, close encounters between individual masses are more important dynamically than for larger N [5]. For this reason, N-body simulators interested in exploring the physics of the N-body problem for larger N often suppress the effects of close encounters artificially by replacing the true $1/r$ potential by a softened potential $V(r) \propto (r^2+\epsilon^2)^{-1/2}$ for some ''softening parameter'' ϵ. This certainly suppresses encounters with impact parameters $<\epsilon$ which, presumably, is a good thing. However, there are strong indications [7] that orbits integrated with such a softened potential tend to be ''less chaotic'' in their behavior, so that the introduction of softening also has the potentially undesirable effect of removing N-body chaos that really ought to be present, even for very large N. In any event, earlier investigations of chaos in the N-body problem based on simulations that incorporate a large amount of softening must be viewed with suspicion, since such simulations could suppress precisely the effects that one might wish to explore.

The role of softening is also related closely to any effort to provide a rigorous justification for a gravitational mean-field theory. The natural approach to this problem would entail considering a collection of N masses with finite ''size'' ϵ and studying the double limit $N\to\infty$ and $\epsilon\to 0$. The obvious point, then, is that the conclusions of such an analysis could well depend on the order in which these (highly singular) limits are taken. To the extent that a nonzero ϵ suppresses chaos, one may envision a situation in which taking the limit $\epsilon\to 0$ first yields orbits that remain chaotic whereas taking the limit $N\to\infty$ first yields orbits that have a vanishing Lyapunov exponent.

This paper summarizes a detailed exploration of chaos in time-independent potentials generated by sampling the smooth density $\rho(\mathbf{r})$ associated with a time-independent solution to the CBE to create a frozen N-body realization of that equilibrium. Most of the work focuses on the particularly simple case of an integrable Plummer potential [5], which derives from a spherically symmetric mass distribution. However, it was also confirmed that, modulo one point discussed in the concluding section, the same qualitative results obtained for the potential associated with a constant density spherical configuration.

In certain respects, this paper complements a recent paper by Valluri and Merritt [8], which considered similar issues, albeit from a somewhat different perspective. As does the present paper, that paper concluded that, in the absence of softening, the Lyapunov exponent χ is not a decreasing function of N, but they did not investigate how a nonzero ϵ may alter this basic conclusion. They too noted that, as N increases, orbits in a frozen-N potential become progressively smoother, but they did not effect detailed comparisons between frozen-N orbits and characteristics in the corresponding smooth potential, or attempt to quantify the rate at which frozen-N orbits and smooth characteristics diverge. In this sense, they did not provide an estimate as to the time scale over which frozen-N orbits and smooth characteristics remain ''close'' in a pointwise sense. Neither did they ascertain whether the divergence of frozen-N orbits and smooth characteristics proceeds exponentially or as a power law in time. They did probe the effects of graininess on collisionless invariants by examining visually how, after a fixed time $\approx 20 t_D$, the root-mean-squared variations in a suitably chosen invariant scale with N, but they did not consider such issues as the sharpness of the orbital power spectrum, which has important implications for the susceptibility of orbits towards various sorts of perturbations.

Section II begins by describing the numerical experiments that were performed. Section III summarizes a computation of honest Lyapunov exponents in frozen N-body realizations of the Plummer potential, exploring how the largest exponent χ associated with representative initial conditions varies as a function of ϵ and N. The principal conclusion here is that, at least for small values of ϵ, orbits in such potentials are invariably chaotic; and that, even for a particle number as large as $N=10^{5.5}$, there is no sense in which increasing N ''turns the chaos off.'' Section IV demonstrates that, even though the Lyapunov exponents do not decrease with increasing N, there is a well-defined sense in which, as N increases, orbits in frozen-N potentials remain ''close to'' smooth potential characteristics with the same initial condition for progressively longer times. Section V concludes by summarizing the basic conclusions, providing a simple physical interpretation, and then commenting on potential implications.

The principal conclusion of this paper is that, for integrable smooth potentials that admit no chaos, the continuum limit makes sense even at the level of pointwise properties of individual trajectories. N-body trajectories and smooth po-

tential characteristics exhibit only a modest power-law divergence, and there exists a time scale $\sim N^{1/2}t_D$ over which orbits in a frozen-N potential remain close to characteristics in the corresponding smooth potential. The possibility of chaotic characteristics leads necessarily to very different behavior and, for this reason, the case of nonintegrable potentials that admit both regular and chaotic characteristics will be considered in a separate paper.

II. DESCRIPTION OF THE NUMERICAL EXPERIMENTS

The numerical computations reported here were performed for a so-called Plummer potential [5],

$$\Phi(r) = -\frac{GM}{\sqrt{r^2+b^2}}. \tag{2.1}$$

This potential is generated via Poisson's equation from a density profile

$$\rho(r) = \left(\frac{3M}{4\pi b^3}\right)\left(1+\frac{r^2}{b^2}\right)^{-5/2}, \tag{2.2}$$

and corresponds to an equilibrium solution to the CBE satisfying

$$f(E) = \begin{cases} A(-E)^{7/2}, & \text{if } \Phi(r=0) < E = \frac{1}{2}v^2 + \Phi < 0; \\ 0, & \text{if } E = \frac{1}{2}v^2 + \Phi > 0. \end{cases} \tag{2.3}$$

Units were so chosen that $G=M=b=1$.

The principal aim was to compare orbits generated in the smooth potential with orbits evolved in time-independent N-body realizations of the potential. For a variety of fixed values of N and ϵ, 20 different time-independent N-body potentials were constructed. Each of these was associated with a random sampling of the smooth density distribution generated using a von Neumann rejection algorithm (cf. [9]). This entailed constructing singular density distributions

$$\rho_N(\mathbf{r}) = \frac{M}{N}\sum_{i=1}^{N}\delta_D(\mathbf{r}-\mathbf{r}_i), \tag{2.4}$$

which, allowing for a softening parameter ϵ, yielded potentials of the form

$$\Phi_N(\mathbf{r}) = -\frac{GM}{N}\sum_{i=1}^{N}\frac{1}{\sqrt{(\mathbf{r}-\mathbf{r}_i)^2+\epsilon^2}}. \tag{2.5}$$

The objective then was to select individual initial conditions $(\mathbf{r}_0,\mathbf{v}_0)$ and to evolve these same initial conditions in both the smooth potential and each of the 20 ''frozen'' N-body potentials, while simultaneously tracking the evolution of a small initial perturbation, periodically renormalized at fixed intervals δt, so as to extract an estimate of the largest (short-time) Lyapunov exponent [10]. A comparison of the 20 orbit

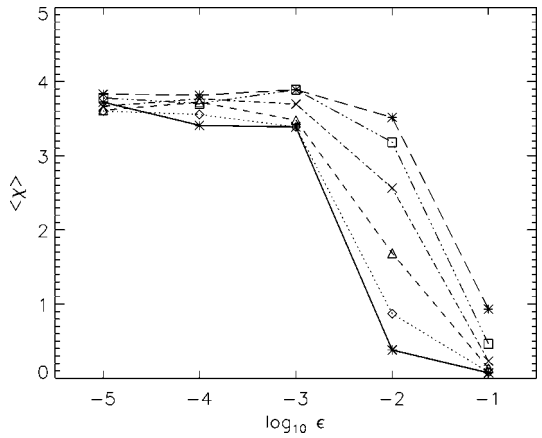

FIG. 1. Mean short-time Lyapunov exponent $\langle\chi\rangle$ as a function of softening parameter ϵ for $N=10^5$ (solid line), $N=10^{4.5}$ (dotted), $N=10^4$ (dashed), $N=10^{3.5}$ (dot-dashed), $N=10^{3.0}$ (triple-dot dashed), and $N=10^{2.5}$ (broad dashed). The integrations were all performed for a single ''typical'' initial condition.

''ensembles'' generated from the 20 different frozen-N potentials with the smooth potential characteristic with the same initial condition facilitated a quantitiative characterization of the average rate at which N-body orbits diverge from orbits in the smooth potential.

The integrations were performed for a time corresponding physically to $\sim 100t_D$ using a Runge-Kutta integrator that typically conserved energy to at least one part in 10^4. The value $100t_D$ was selected (i) because it corresponded to an interval sufficiently long that one began to see convergence towards a well-defined Lyapunov exponent χ and, perhaps more importantly, (ii) because, for physical systems like real galaxies, $100t_D$ corresponds to an interval comparable to the age of the Universe.

The total particle number N in the ''frozen'' N-body potentials was allowed to vary between $N=10^{2.5}$ and $N=10^{5.5}$. Physical interest focuses primarily on the limit $\epsilon \to 0$, this corresponding to an ''honest'' N-body calculation. However, for reasons described already, the effects of a nonzero ϵ were also considered in some detail.

III. SHORT-TIME LYAPUNOV EXPONENTS

The principal diagnostic here was the mean (short-time) Lyapunov exponent $\langle\chi\rangle$, generated, for a given choice of initial condition and for specified values of ϵ and N, as the average value of χ at $t=100t_D$ for 20 different frozen-N potentials. The fundamental question was how, for a fixed initial condition, this $\langle\chi\rangle$ depends on ϵ and N. Figure 1 exhibits $\langle\chi\rangle$ as a function of $\log_{10}\epsilon$ for multiple integrations of one representative initial condition, with radial and tangential velocities comparable in magnitude [11], allowing for several different values of N. Figure 2 gives $\langle\chi\rangle$ as a function of $\log_{10}N$ for the same initial condition, now allowing for several different values of ϵ. It is evident from Fig. 1 that, at least for comparatively large values of softening parameter, decreasing ϵ tends to make the orbit more chaotic. This is hardly surprising: Since the smooth potential is integrable,

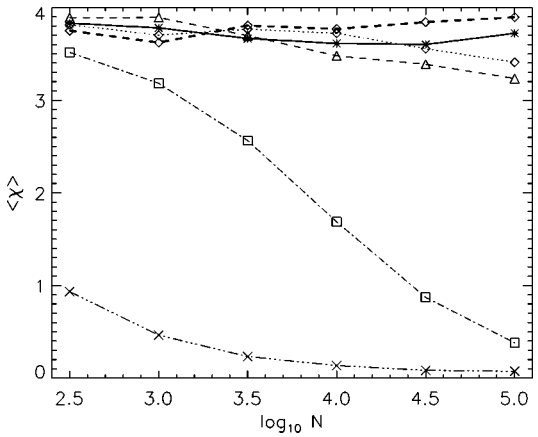

FIG. 2. Mean short-time Lyapunov exponent $\langle\chi\rangle$ as a function of particle number N for $\epsilon=10^{-5}$ (solid line), $\epsilon=10^{-4}$ (dotted), $\epsilon=10^{-3}$ (thin-dashed), $\epsilon=10^{-2}$ (dot-dashed), and $\epsilon=10^{-1}$ (triple-dot dashed), all computed for the initial condition used to generate Fig. 1. The short time $\langle\chi\rangle$ for a different initial condition corresponding to a smooth radial orbit, again evolved with $\epsilon=10^{-5}$, is indicated by the curve with thick dashes.

one anticipates that the chaos is associated completely with close encounters between the test mass and individual frozen masses. The introduction of a nonzero smoothing corresponds *de facto* to the introduction of a minimum impact parameter (since the potential is bounded in magnitude by $V_{max}=-GM/N\epsilon$) but the existence of such a minimum impact parameter limits the maximum effect that can arise from a close encounter.

However, for sufficiently small values of ϵ, the precise value of ϵ appears to be largely immaterial. This again is hardly surprising: As long as ϵ is small compared with the value of the closest separation between the test particle and any of the frozen particles during the course of the integration, the test particle feels an essentially unsoftened potential and should behave (at least statistically) as if $\epsilon=0$. The point then is that, for $N\leqslant 10^6$ and an integration time as short as $100t_D$, the minimum separation associated with the closest encounter between the test mass and any of the frozen masses should be greater than or comparable to $\epsilon\sim 10^{-4}$. Indeed, a simple geometric argument indicates [12] that the time scale t_ϵ for a close encounter with minimum separation as small as ϵ scales as

$$\frac{t_\epsilon}{t_D}\sim\frac{1}{N}\left(\frac{R_{sys}}{\epsilon}\right)^2, \tag{3.1}$$

where R_{sys} is the size of the system in question.

One obvious implication of these results is that the introduction of a large amount of softening into a numerical simulation may have the unnatural result of significantly decreasing the amount of chaos manifested by individual orbits in a real astronomical system.

For comparatively large values of ϵ, $\langle\chi\rangle$ decreases rapidly with increasing N but, for sufficiently small values of ϵ, it appears that $\langle\chi\rangle$ is nearly independent of N (although there are hints that $\langle\chi\rangle$ may continue to *increase* very slowly). That, for large ϵ, $\langle\chi\rangle$ should decrease with increasing N may again be explained by comparing the magnitude of ϵ with the typical distance between masses in the system, which is of order $n^{-1/3}\sim R_{sys}/N^{1/3}$, with n a characteristic number density. If ϵ is larger than, or comparable to $n^{-1/3}$, even weak close encounters are essentially ''turned off,'' so that the source of chaos has been largely reduced, if not completely removed. The fact that $\langle\chi\rangle$ should be essentially independent of N in the limit $\epsilon\rightarrow 0$ has been argued by various authors in a number of different ways [2,3]. A simple physical explanation is provided in the concluding section.

If a single orbit be integrated for progressively longer times, how quickly will the short-time Lyapunov exponent $\chi(t)$ converge towards the true time-independent χ? Studies of orbits in smooth nonintegrable potentials reveal that, when the phase space is highly complex and, because of the Arnold web, orbits may be ''stuck'' temporarily in regions where the short-time Lyapunov exponents are especially small or especially large, the time required for a reasonable level of convergence may be extremely long, $\sim 10^5 t_D - 10^6 t_D$ or even more [10]. If, however, the phase space is simpler in the sense that the Arnold web forms less of an impediment and such trapping is comparatively rare, the time required is typically much shorter. One way in which to quantify the overall rate of convergence is by performing a simple time series analysis: An orbit segment of length T may of course be divided into k segments of length $\Delta t=T/k$ and a short-time Lyapunov exponent $\chi(\Delta t)$ computed for each segment. The dispersion $\sigma_\chi(\Delta t)$ then provides a useful probe of the degree to that, on time scales $\sim\Delta t$, the degree of chaos exhibited by different orbit segments is more or less the same. Determining σ_χ as a function of Δt provides a quantitative characterization of the rate of convergence towards a unique χ_∞. A simple argument based on the central limits theorem suggests [13] that, if the accessible phase-space regions are simple and trapping is rare, so that the amounts of chaos manifested at times t and $t+\Delta t$ are essentially uncorrelated,

$$\sigma_\chi\propto(\Delta t)^{-p}, \tag{3.2}$$

with $p=1/2$. If, alternatively, the phase space is complex and trapping is important, one would expect that σ_χ decreases much more slowly with increasing Δt.

Such a time series analysis was performed for the data sets used to generate the mean exponents $\langle\chi\rangle$. For each set of 20 integrations, each orbit segment of length $T=100t_D$ was separated into k segments of length $\Delta t=T/k$. A short-time Lyapunov exponent $\chi(\Delta t)$ was then computed for each of the resulting $20k$ segments, and these were used to compute the dispersion $\sigma_\chi(\Delta t)$. Allowing for $k=2^q$, for $q=0$, 1, 2, 3, 4, 5, and 6 was equivalent to varying Δt between $\Delta t=(100/64)t_D$ and $\Delta t=100t_D$. This time-series analysis led to the conclusion that the dispersion σ_χ is typically well fit by a power-law dependence of the form given by Eq. (3.2), although the exponent p tends to be somewhat smaller than $p=1/2$, the best-fit value typically satisfying $p\sim 0.4$. Several examples are exhibited in Fig. 3. The fact that p is comparatively close to 1/2, rather than the much smaller values that

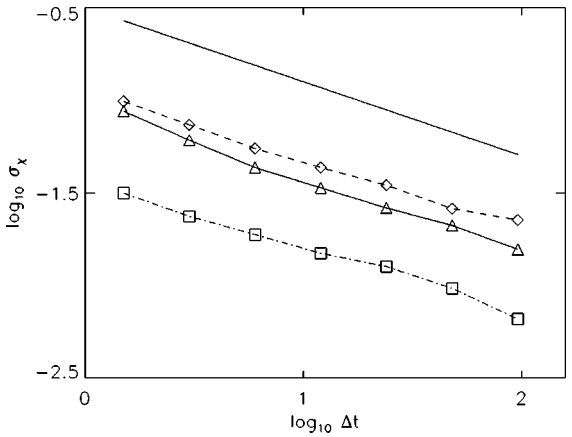

FIG. 3. $\log_{10}\sigma_\chi(\Delta t)$ as a function of $\log_{10}\Delta t$ for three sets of simulations: $N=31\,623$ and $\epsilon=0.0001$ (solid curve), $N=316$, and $\epsilon=0.0001$ (dashed curve), and $N=316$ and $\epsilon=0.1$ (dot-dashed curve), all computed for the initial condition used to generate Fig. 1. The thick solid line has a slope corresponding to $p=0.4$.

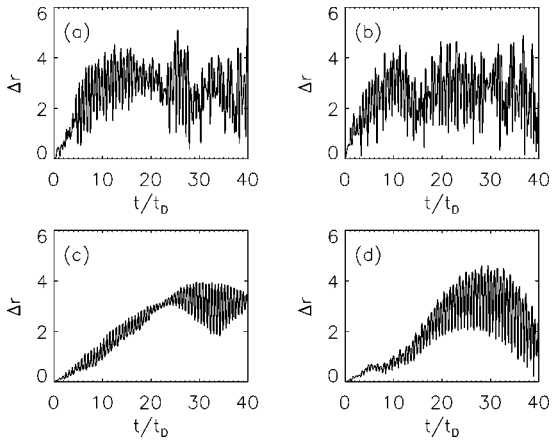

FIG. 4. (a) The deviation $\Delta r=|\mathbf{r}-\mathbf{r}_s|$ from the smooth potential characteristic for one representative frozen-N orbit evolved with $\epsilon=10^{-4}$ and $N=1000$ for the initial condition used to generate Fig. 1. (b) Another frozen-N orbit evolved with the same ϵ and N for the same initial condition. (c) and (d) The same for $N=100\,000$.

are often observed in very ''sticky'' nonintegrable potentials [13], corroborates the intuition that, because the chaos in this problem is associated exclusively with close encounters, trapping is rare and the degree of chaos exhibited at different times tends to be statistically uncorrelated.

IV. COMPARISON OF SMOOTH AND *N*-BODY ORBITS

It is clear that, for sufficiently short times, a frozen-N orbit will coincide almost exactly with the smooth potential characteristic associated with the same initial condition. And similarly, it is clear that, at sufficiently late times, the irregularities in the frozen-N potential will cause the frozen-N orbit to deviate significantly from the smooth characteristic. Probing the validity of the continuum limit at the level of individual orbits thus devolves into determining the rate at which the frozen-N orbits and smooth characteristics diverge. In this connection, two obvious questions arise. Do frozen-N orbits diverge from the smooth characteristics exponentially or as a power law in time? And how does the overall rate of divergence depend on N?

Such probes of the validity of the continuum limit differ from the ordinary point of view, where convergence is typically defined in terms of quantities like bulk moments of the system, ignoring completely the behavior of individual trajectories. A possible intermediate characterization is to focus *not* on the pointwise behavior of the chaotic orbits but, instead, on quantities that might be less sensitive to the N-body chaos. In particular, one may also ask: How do frozen-N orbits deviate from smooth characteristics in terms of quantities that, in the smooth potential, correspond to time-independent constants of the motion, like angular momentum in a spherically symmetric system?

These questions were addressed here both visually and quantitatively through a computation of the statistical properties of frozen-N orbits. Given $n=20$ different trajectories $\{(\mathbf{r}_i(t),\mathbf{v}_i(t))\}$, $i=1,\ldots,n$, and the smooth characteristic $(\mathbf{r}_s(t),\mathbf{v}_s(t))$ associated with the same initial condition, there are two types of moments that one might choose to consider. Quantities such as

$$\langle\mathbf{r}\rangle=\frac{1}{n}\sum_{i=1}^{n}\mathbf{r}_i \tag{4.1}$$

and

$$Dr^2=\langle|\mathbf{r}_i-\langle\mathbf{r}\rangle|^2\rangle\equiv\frac{1}{n}\sum_i|\mathbf{r}_i-\langle\mathbf{r}\rangle|^2, \tag{4.2}$$

and the corresponding quantities generated from $\mathbf{v}$ and $\mathbf{J}=\mathbf{r}\times\mathbf{v}$ focus on the frozen-N orbits in and of themselves. Alternatively, such moments as

$$\Delta r^2\equiv\langle|\mathbf{r}-\mathbf{r}_s|^2\rangle=\frac{1}{n}\sum_i|\mathbf{r}_i-\mathbf{r}_s|^2 \tag{4.3}$$

and

$$\delta r^2=\langle|\langle\mathbf{r}\rangle-\mathbf{r}_s|^2\rangle \tag{4.4}$$

compare the frozen-N orbits with the smooth potential characteristic and, as such, their behavior as a function of N is particularly relevant in understanding the continuum limit. Overall, the quantities Dr, δr, and Δr were found to exhibit comparatively similar evolutions, so that attention below focuses on the moments $\langle\mathbf{r}\rangle$ and Δr, which seem especially natural physically.

The most striking conclusion is that individual frozen-N orbits typically diverge from the smooth characteristic as a power law in time, *not* exponentially [17]. This is true both for comparatively large values of ϵ, where the frozen-N orbits are nearly regular, and for smaller values of ϵ, where the orbits are much more chaotic. This result is perhaps surprising. One might naively have supposed that, since the frozen-N orbits are strongly chaotic, at least for small ϵ, they would tend to diverge exponentially from the smooth characteristics on a time scale $\tau\sim\chi^{-1}$. However, such an exponential divergence is most definitely *not* observed.

Figure 4 exhibits the quantity $\Delta r\equiv|\mathbf{r}-\mathbf{r}_s|$ for representa-

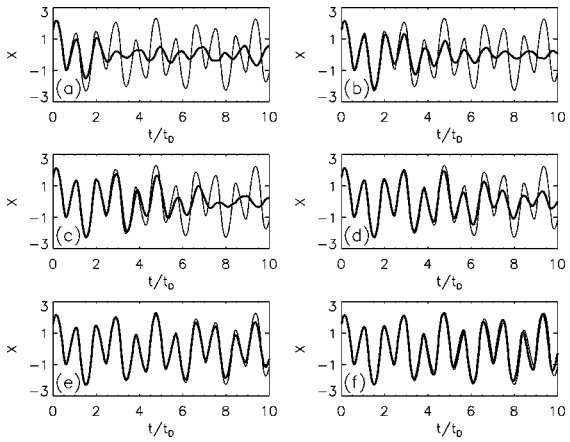

FIG. 5. (a) The trajectory $x_s(t)$ in the smooth potential (thin curve) and the mean trajectory $\langle x(t)\rangle$ (thick curve) derived from 20 frozen-N simulations with $N=316$ and $\epsilon=10^{-4}$, performed for the initial condition used to generate Fig. 1. (b) The same for $N=1000$. (c) $N=3162$. (d) $N=10\,000$. (e) $N=31\,623$. (f) $N=100\,000$.

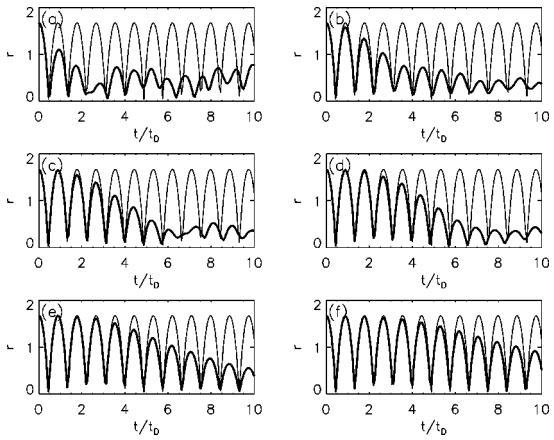

FIG. 6. (a) The radial coordinate $r_s(t)$ in the smooth potential (thin curve) and the mean trajectory $\langle r(t)\rangle$ (thick curve) derived from 20 frozen-N simulations with $N=316$ and $\epsilon=10^{-4}$, performed for an initial condition corresponding in the smooth potential to a purely radial orbit. (b) The same for $N=1000$. (c) $N=3162$. (d) $N=10\,000$. (e) $N=31\,623$. (f) $N=100\,000$.

tive frozen-N orbits evolved with $\epsilon=10^{-4}$ from the same initial condition used to generate Fig. 1. The first two panels are for $N=1000$; the latter two for $N=100\,000$. It is evident that, rather than exponential, the growth of Δr is roughly linear in time.

For how long does this power-law divergence persist? Does it cease when the distance between the frozen-N orbit and the smooth characteristic is still small, or does the divergence continue until the frozen-N orbit and the smooth characteristic tend to be widely separated in configuration space? If, e.g., this divergence terminated at comparatively small separations, much smaller than the size of the system, one could argue that, even though the frozen-N orbits are chaotic, they still remain ''close'' to the smooth characteristics. The answer here is that this divergence continues until the typical separation has become comparable to the size of the configuration-space region to which the orbits are confined and the frozen-N orbit has become completely ''decorrelated'' in appearance from the smooth potential characteristic.

The same conclusion is also obtained if one averages over 20 orbits generated in different frozen-N potentials (with the same ϵ and N) from the same initial condition. The six panels of Fig. 5, generated for the initial condition used in Figs. 1–3, compare $\langle x\rangle$ for such frozen-N ensembles with the smooth x_s for orbits evolved with $\epsilon=10^{-5}$, allowing for six values of N extending from $N=316$ to $N=100\,000$. In each case, one finds that, for sufficiently large t, $\langle x\rangle\to 0$, as would be expected if the frozen-N orbits have become completely different from one another and move through configuration space with random orientations. Figure 6 compares the radial coordinates $\langle r\rangle$ and r_s for the extreme case of an initial condition corresponding in the smooth potential to a purely radial orbit [18].

The time scale t_G on which the frozen-N orbits diverge from the smooth characteristic, and hence, the time scale on which Δr grows, increases with increasing N. Even though the frozen-N orbits remain ''equally chaotic'' in the sense that their Lyapunov exponents χ remain nearly constant, they remain close to the smooth characteristic for progressively longer times.

The left-hand panels of Fig. 7 exhibit $\Delta r/(2^{1/2}R_s)$, with R_s^2 the mean value of r^2 associated with the smooth characteristic, as computed for the same initial condition evolved with $\epsilon=10^{-4}$ for $N=1000$ and $N=100\,000$. The right-hand side exhibits the same data, recorded at intervals of $0.025t_D$, once they have been subjected to a boxcar averaging over an interval $\delta t=1.0t_D$. The large envelops associated with the curves in the left-hand panels reflect, e.g., the fact that, at late times, individual orbits in the $n=20$ orbit ensembles are oscillating about a value of unity.

That $\Delta r/(2^{1/2}R_s)$ converges towards unity is a reflection of the fact that the orbits have indeed become completely different from one another: Given that the frozen-N orbits

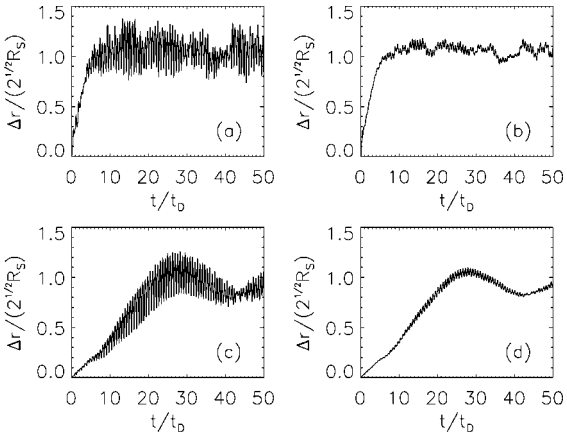

FIG. 7. (a) The quantity $\Delta r/\sqrt{2R_s^2}$ for frozen-N simulations with $N=1000$ and $\epsilon=10^{-4}$. (b) The same data subjected to boxcar averaging over an interval $t=t_D$. (c) and (d) The same for $N=100\,000$.

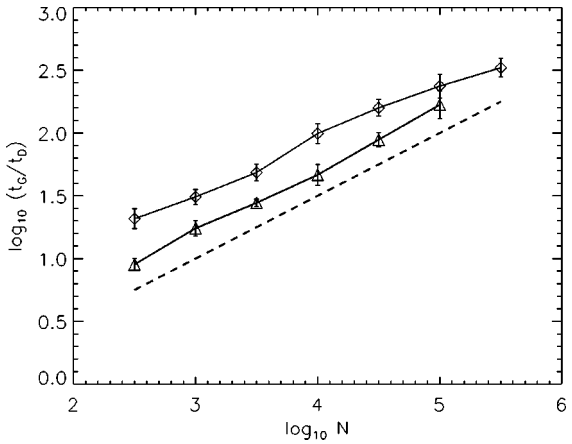

FIG. 8. Best-fit values of the time scale $t_G(N)$ associated with the divergence of smooth and frozen-N orbits for two different initial conditions: $\Delta r/R_s=\Delta v/V_s\equiv t/t_G$. The dashed line has slope 1/2, corresponding to an $N^{1/2}$ dependence.

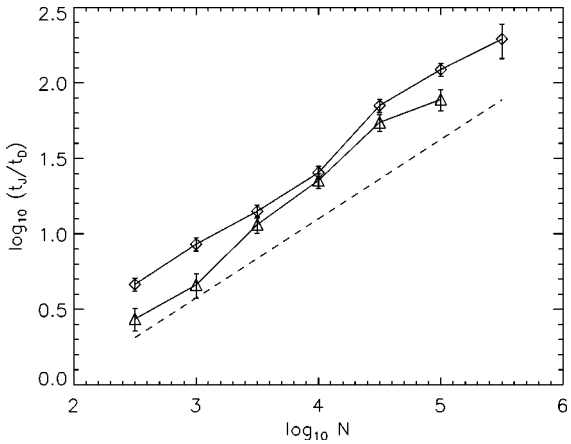

FIG. 9. Best-fit values of the time scale $t_J(N)$ associated with changes in angular momentum for frozen-N orbits for two different initial conditions: $\Delta J^2/J_s^2\equiv t/t_J$. The dashed line has slope 1/2, corresponding to an $N^{1/2}$ dependence.

conserve energy, one might expect that their average distance from the origin should, on average, be the same as for the smooth characteristic, so that

$$\langle r^2(t)\rangle\rightarrow R_s^2 \quad \text{for} \quad t\rightarrow\infty. \tag{4.5}$$

Assuming, however, that this is true and that

$$\langle \mathbf{r}(t)\cdot\mathbf{r}_s(t)\rangle\rightarrow 0 \quad \text{for} \quad t\rightarrow\infty, \tag{4.6}$$

one infers that $\Delta\mathbf{r}^2\rightarrow 2R_s^2$. Analogous behavior is observed for the quantity $\Delta v/2^{1/2}V_s$, with V_s^2 defined correspondingly for the smooth characteristic.

As is manifested by Fig. 7, the growth of Δr and Δv is roughly linear in time. Indeed, when comparing an ensemble of frozen-N orbits with a smooth orbit characteristic generated from the same initial condition, one finds that, for small ϵ, Δr and Δv are both reasonably well fit by a linear growth law of the form

$$\frac{\Delta r}{r_s}=\frac{\Delta v}{v_s}=\frac{t}{t_G}. \tag{4.7}$$

The growth time t_G, which is the same for both Δr and Δv, satisfies

$$t_G\approx A_G N^p t_D, \tag{4.8}$$

with A_G of order unity and $p\approx 1/2$. Figure 8 exhibits $\log_{10}(t_G/t_D)$ as a function of $\log_{10}N$ for two different initial conditions evolved with $\epsilon=10^{-5}$.

The fact that t_G scales as $N^{1/2}$ would suggest that the divergence of the frozen-N orbits from smooth characteristics reflects a diffusion process, associated with a collection of random close encounters. However, this might in turn suggest that Δr and Δv should grow as $t^{1/2}$, rather than the approximately linear growth that was observed in the numerical simulations. Interesting, though, such a $t^{1/2}$ behavior is obtained for quantities such as angular momentum, which are conserved absolutely in the smooth potential. Indeed, one finds that, for small ϵ, ΔJ satisfies

$$\frac{\Delta J^2}{J_s^2}=\frac{t}{t_J}, \tag{4.9}$$

where J_s is the typical magnitude of the angular momentum associated with a characteristic with the specified energy. The growth time t_J again scales as $N^{1/2}$, but tends to be somewhat larger than t_G, so that

$$t_J\approx A_J N^p t_D, \tag{4.10}$$

with $A_J\sim 3A_G$ and $p\approx 1/2$. Figure 9 exhibits $\log_{10}(t_J/t_D)$ as a function of $\log_{10}N$ for the same integrations used to generate Fig. 8.

There is also a clear visual sense in which, as N increases, the frozen-N orbits become progressively more regular in appearance. This is, e.g., evident in Fig. 10, which exhibits the x-y projections of representative frozen-N orbits with N varying between $N=316$ and $N=316\,228$, all generated from the same initial condition and integrated for a time $t=25t_D$ with $\epsilon=10^{-5}$. The final panel exhibits the smooth characteristic associated with the same initial condition. The most obvious point is that, as N increases, the configuration-space region to which the orbit is restricted more closely coincides with the region occupied by the characteristic. For example, only for the three largest values of N is the orbit ''centrophobic'' in the same sense as the characteristic. The lower-left panel of Fig. 1 in Valluri and Merritt [8] exhibits similar data for an orbit that, in the continuum limit, becomes [5] a regular ''box'' rather than a ''tube.''

Also evident is the fact that the orbit ''looks smoother'' for larger values of N. This visual impression reflects the fact that, as N increases, the power associated with the Fourier spectrum of an orbit tends to become more concentrated near a few special frequencies. (Since the smooth orbit associated with the same initial condition is regular, all its power is concentrated at a countable set of discrete frequencies.) This

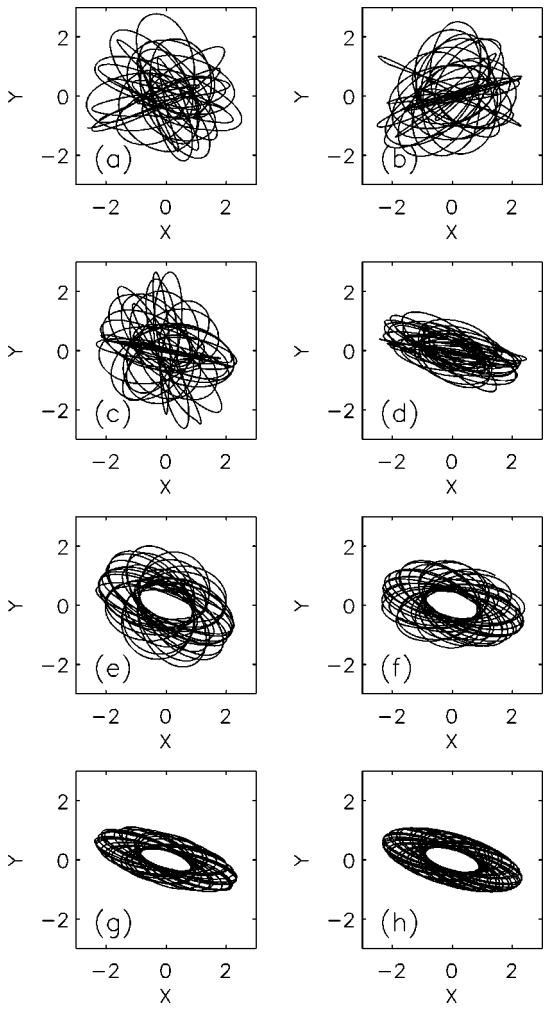

FIG. 10. The x-y projection of representative frozen-N orbits generated from the same initial condition, evolved for $t=25t_D$ with $\epsilon=10^{-5}$. (a) $N=316$. (b) $N=1000$. (c) $N=3163$. (d) $N=10\,000$. (e) $N=31\,623$. (f) $N=100\,000$. (g) $N=316\,228$. (h) The x-y projection of the same initial condition evolved in the smooth potential.

trend is illustrated in the eight panels of Fig. 11, each of which exhibits $|x(\omega)|$ for a single frozen-N orbit generated from the same initial condition. In each case, the data are so normalized that the peak frequency has $|x(\omega)|=1$. The spectra were generated from a time series of 4001 points, recorded at intervals of $0.025t_D$.

The degree to which the orbits become more nearly regular with increasing N may be quantified by determining [14] the ''complexity'' of the orbits, i.e., the number of frequencies in the discrete Fourier spectrum that contain an appreciable amount of power. Two such measures of complexity are illustrated in Fig. 12, which was computed for ensembles of frozen-N orbits with varying N, all evolved with $\epsilon=10^{-5}$ and generated from the same initial condition. The solid curve exhibits $f_{0.1}$, defined as the sum of the numbers of frequencies $f_{0.1,x}$, $f_{0.1,y}$, and $f_{0.1,z}$, which have more than 10% as much power as the peak frequencies for ω_x, ω_y, and ω_z, i.e.,

$$f_{0.1}=f_{0.1,x}+f_{0.1,y}+f_{0.1,z}. \tag{4.11}$$

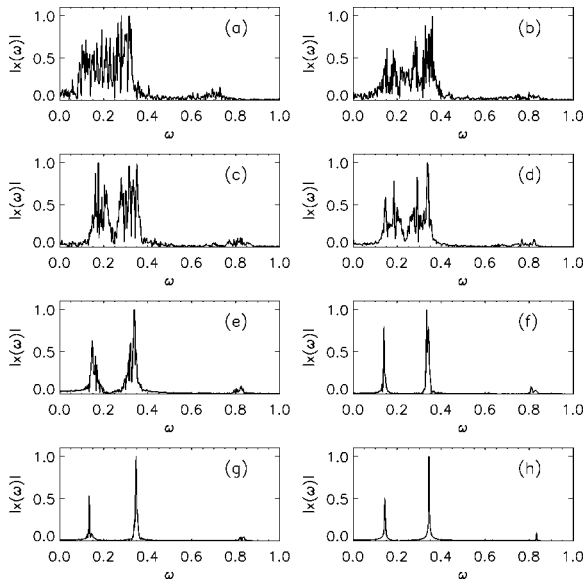

FIG. 11. (a) The Fourier transformed $|x(\omega)|$ for one frozen-N integration of the initial condition used to generate Fig. 4, evolved with $\epsilon=10^{-5}$ and $N=316$. (b) The same for $N=1000$. (c) $N=3162$. (d) $N=10\,000$. (e) $N=31\,623$. (f) $N=100\,000$. (g) $N=316\,228$. (h) $|x(\omega)|$ for a characteristic in the smooth potential with the same initial condition, with data recorded at the same intervals for the same total integration time.

The dashed curve exhibits $k_{0.95}$, defined correspondingly as the sum of the numbers of frequencies required to capture 95% of the power in the x, y, and z directions. In each case, the curve represents an average over different orbits in the ensemble, and the error bars represent the associated dispersions. The obvious point is that both these quantities decrease with increasing N.

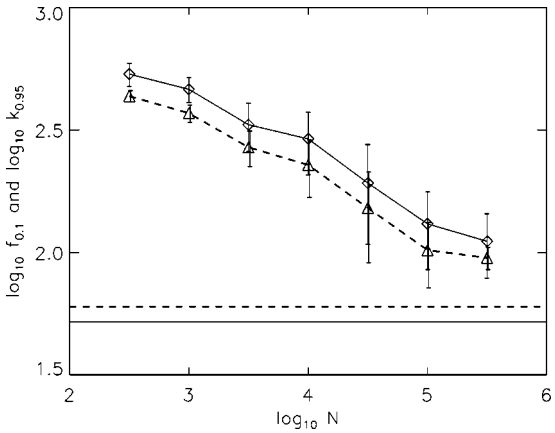

FIG. 12. Two probes of the complexity of frozen-N orbits for an ensemble of orbits with the same initial condition evolved with $\epsilon=10^{-5}$. The solid curve exhibits $f_{0.1}$, the number of frequencies that have power equal to at least 10% of the power in the peak frequencies. The dashed curve exhibits $k_{0.95}$, the number of frequencies required to capture 95% of the total power. The horizontal lines show $f_{0.1}$ and $k_{0.95}$ for a smooth characteristic generated identically from the same initial condition, thus exhibiting the intrinsic limitations associated with the discrete time series of data points.

The fact that, as N increases, power becomes more concentrated near a few special frequencies has important implications for various physical processes that rely on resonances. For example, a variety of recent arguments in both galactic and solar system dynamics invoke a process of so-called ''resonant relaxation'' [15], which relies on the assumption that, in the presence of a large central object (a supermassive black hole in the center of a galaxy or the Sun at the center of the solar system), N-body orbits behave very nearly as if they were Keplerian trajectories in the fixed $1/r$ potential associated with the central object. If the chaos exhibited by individual orbits [16] implied that these orbits were highly irregular, so that their power was not concentrated near the special Keplerian frequencies, resonant relaxation might seem quite implausible. Given, however, that the orbits become progressively more regular for increasing N, resonant relaxation would seem eminently reasonable, at least for systems in which N is sufficiently large.

Alternatively, one might be concerned with the response of orbits to nearly random perturbations, reflecting, e.g., an external environment. In this case, perturbation act generically via a resonant coupling between the natural frequency of frequencies of the perturber and the natural frequencies of the orbit [20] so that, in agreement with simulations [21], one might expect generically to see larger effects for orbits with broader band Fourier spectra. The crucial point, then, is that, even though frozen-N orbits remain chaotic in the sense that their Lyapunov exponents do not decrease in magnitude, they become more regular in the sense that their power spectra become more sharply peaked.

The fact that N-body orbits may have both a large positive Lyapunov exponent and a comparatively sharp Fourier spectrum has profound implications for the meaning of chaos in N-body systems. In the context of time-independent Hamiltonian systems, it is customary [22] to consider positive Lyapunov exponent and aperiodicity (and hence, continuous Fourier spectrum) as two complementary notions of chaos; and, at least for smooth lower-dimensional systems, there is often a strong correlation between the size of the largest short-time Lyapunov exponent and the Fourier complexity associated with chaotic orbit segments [14]. That orbits in frozen-N potentials may have large Lyapounov exponents but still be nearly periodic suggests strongly that the chaos observed here is fundamentally different from the chaos associated with a bulk nonintegrable potential.

V. CONCLUSIONS AND DISCUSSION

Although trajectories remain chaotic in the sense that the largest Lyapunov exponent does not decrease towards zero, there is a clear sense in which, for increasing N, orbits in frozen-N potentials exhibit a pointwise convergence towards characteristics in the smooth potential that the frozen-N potentials sample. Viewed in configuration or velocity space, frozen-N orbits tend to diverge linearly from the smooth characteristic with the same initial condition on a time scale t_G that is proportional to $N^{1/2}$. Contrary to earlier speculations, N-body trajectories and smooth characteristics do *not* diverge exponentially on a time scale $\tau \sim \chi^{-1} \sim t_D$. In this sense, the continuum limit appears justified even at the level of individual trajectories, at least for times $t \ll N^{1/2} t_D$. The fact that frozen-N orbits remain chaotic for very large N is completely consistent with the existence of a well-defined continuum limit.

It is easy to understand qualitatively why the frozen-N orbits should remain chaotic even for very large N. Given that the chaos disappears completely in the continuum limit, where the orbits reduce to integrable characteristics, it would seem clear that the chaos must be associated with a sequence of ''random'' interactions between a ''test'' particle and a collection of ''field'' particles. However, this would suggest that the time scale associated with the growth of a small initial perturbation may be estimated by considering the tidal effects associated with a pair of particles separated by a distance comparable to the typical interparticle separation. This tidal acceleration will of course scale as

$$\delta\ddot{\mathbf{r}} = (\delta\mathbf{r}\cdot\boldsymbol{\nabla})\mathbf{a} \sim \frac{Gm}{r^3}\delta\mathbf{r}, \tag{5.1}$$

with r the separation and m the particle mass. Given, however, that $r \sim n^{-1/3} \sim N^{-1/3} R_{sys}$, with n a characteristic number density and R_{sys} the size of the system, it follows that the time scale t_* associated with the interaction should satisfy

$$t_* \sim 1/\sqrt{G\rho}. \tag{5.2}$$

In other words, the time scale associated with any orbital instability induced by the graininess of the system should be comparable to the dynamical time t_D, seemingly independent of particle number N. As N increases, the size of the individual particle mass m and the cube of the typical separation between particles, $\sim n^{-1}$, both decrease as N^{-1} so that their ratio is independent of particle number [23].

That the chaotic frozen-N orbits appear to become ''more nearly regular'' as N increases is consistent with the observation by Valluri and Merritt [8] that the ''scale'' associated with N-body chaos decreases with increasing N. Specifically, by comparing trajectories associated with two nearby initial conditions evolved in the same frozen-N potential, Valluri and Merritt found (cf. the lower-right hand panel of their Fig. 1) that, when scaled in terms of R_{sys}, the size of the system, the typical separation R_{sat} on which the initial exponential divergence saturates decreases with increasing particle number, so that R_{sat}/R_{sys} is a decreasing function of N. It should be stressed that this ''saturation'' in the exponential divergence of initially nearby N-body trajectories is very different from the diffusive $t^{1/2}$ divergence of frozen-N orbits from smooth potential characteristics, which, seemingly independent of N, only terminates when the typical separation has become comparable to the size of the system.

That the rate of divergence of initially nearby frozen-N orbits in the nonlinear regime slows more and more for larger N may be quantified by tracking the actual evolution of two orbits generated from nearby initial conditions and determining the time required before their separation becomes ''macroscopic.'' The result of such an investigation is illustrated in Fig. 13, which was generated once again from

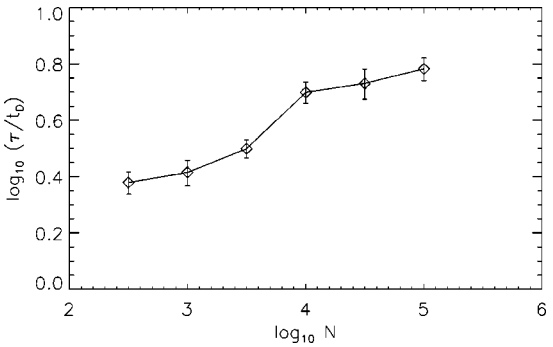

FIG. 13. The mean time required for two frozen-N orbits separated initially by a distance $\delta r = 10^{-6}$ to achieve a macroscopic separation $\delta r = 1$.

ensembles of 20 frozen-N orbits all evolved from the same initial condition with $\epsilon = 10^{-5}$. In each case, the unperturbed orbits were identical to those used to generate Fig. 1; the perturbed orbits involved changing the initial value of x by an amount $\delta x = 10^{-6}$. Figure 13 exhibits as a function of N the mean time τ required before the separation

$$\delta r = (\delta x^2 + \delta y^2 + \delta z^2)^{1/2} \tag{5.3}$$

had achieved the value $\delta r = 1$. (For this initial condition, the average value of r associated with the smooth characteristic was $R_s \approx 1.83$.) The error bars were derived by considering the first and second ten orbits in the ensemble separately. Because individual orbits diverge at vastly different rates, the dispersion associated with a 20 orbit ensemble is much larger than reflected by these error bars. It is clear that τ increases systematically with increasing N, although considerably more slowly than with the $N^{1/2}$ dependence observed for the divergence time scales t_G and t_J.

When viewed in terms of collisionless invariants such as angular momentum, the divergence of frozen-N orbits from smooth characteristics with the same initial condition is well approximated as a diffusion process, in which ΔJ grows as $(t/t_J)^{1/2}$ and where, for fixed t_D, the divergence time scale t_J varies at least approximately as $N^{1/2}$. This reinforces the conventional wisdom [19] that discreteness effects may be modeled as white, or nearly white, Gaussian noise in the context of a Langevin or Fokker-Planck description. It might, therefore, seem somewhat surprising that, although the divergence time scale t_G in configuration or velocity space again scales as $N^{1/2}$, the quantities Δr and Δv grow *linearly* in time, rather than as $t^{1/2}$.

In this regard, it is significant that if the smooth Plummer potential be replaced by the smooth potential associated with a constant density configuration, the linear growth exhibited Δr and Δv is in fact replaced by the ''expected'' diffusive behavior. In this case, Δr and Δv both grow as $t^{1/2}$, and, when expressed in units of the dynamical time t_D, the growth time t_G is somewhat longer, corresponding more nearly to the time scale t_J associated with ΔJ. This is, e.g., evident from Fig. 14, which exhibits Δr^2 for one representative initial condition [24], generated as in Fig. 7, for $N = 1000$ and $N = 100\,000$.

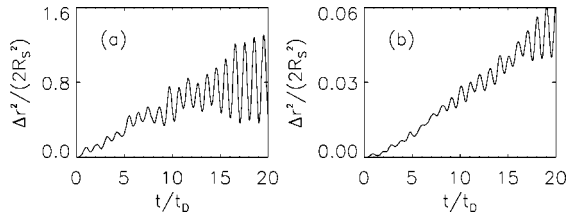

FIG. 14. (a) The quantity $\Delta r^2/2R_s^2$ for frozen-N simulations with $N = 1000$ and $\epsilon = 10^{-4}$, now considering discretizations of a constant density sphere with total mass $M = 1.0$ and radius $R = 4.0$. (b) The same for $N = 100\,000$.

This suggests strongly that the behavior of Δr and Δv observed for the Plummer potential is associated with linear phase mixing. Because of finite number statistics, the same initial condition $(\mathbf{r}_0, \mathbf{v}_0)$ in different frozen-N realizations of a Plummer potential will correspond to somewhat different energies, the values of which are conserved in the subsequent evolution. However, even neglecting discreteness effects, initially proximate orbits in a generic integrable potential will, if their energies be unequal, tend to diverge linearly. For example, two orbits evolved in a smooth Plummer potential with the same initial $\mathbf{r}$ but slightly different values of $\mathbf{v}$ and, hence, slightly different energies, will oscillate with somewhat different frequencies and, as a result, exhibit an overall linear divergence. If, however, the orbits are evolved instead in the potential associated with a constant density distribution, this is no longer true. A constant density sphere corresponds to a harmonic potential, where all orbits have the same unperturbed frequencies; and, for this reason, orbits in the smooth potential with slightly different energies will not exhibit such a systematic divergence.

The fact that frozen-N orbits look ''more nearly regular'' for large N suggests that the chaos associated with discreteness effects in the N-body problem should be viewed very differently from the chaos associated with a bulk nonintegrable potential. When evolved into the future, two nearby chaotic initial conditions in such a potential tend to diverge exponentially until they are separated by a distance comparable to the size of the easily accessible (i.e., not significantly impeded by the Arnold web) connected phase-space region to which the orbits are confined, a region that tends, typically, to be macroscopic. By contrast, the scale associated with chaos induced by discreteness effects in the N-body problem is distinctly microscopic, at least for comparatively large N. It would appear that any single orbit with fixed energy may access a phase-space region that is in fact very large; but the chaos that it experiences is a superposition of short-range effects with characteristic scale $\ll R_{sys}$.

ACKNOWLEDGMENTS

The authors acknowledge useful discussions with Alexei Fridman, Salman Habib, and Ilya Pogorelov. This research was supported in part by NSF AST-0070809 and by the Institute for Geophysics and Planetary Physics at Los Alamos National Laboratory.

[1] R.H. Miller, Astrophys. J. **140**, 250 (1964).
[2] H.E. Kandrup, Physica A **169**, 73 (1989).
[3] J. Goodman, D. Heggie, and P. Hut, Astrophys. J. **415**, 715 (1993).
[4] H.E. Kandrup, M.E. Mahon, and H. Smith, Astrophys. J. **428**, 458 (1994), and references cited therein.
[5] J. Binney and S. Tremaine, *Galactic Dynamics* (Princeton University Press, Princeton, 1987).
[6] Rigorous justifications of mean-field theory, such as the classic paper on gravitating fermions [P. Hertel and W. Thirring, Commun. Math. Phys. **24**, 22 (1971)], typically prove convergence for quantities such as a free energy or some other thermodynamics quantity, which has implications for bulk moments but says absolutely nothing about the behavior of individual orbits.
[7] H.E. Kandrup and H. Smith, Astrophys. J. **374**, 255 (1991).
[8] M. Valluri and D. Merritt, in *The Chaotic Universe*, edited by R. Ruffini and V.G. Gurzadyan (World Scientific, New York, 1999).
[9] S.J. Aarseth, M. Hénon, and R. Wielen, Astron. Astrophys. **37**, 183 (1974).
[10] A.J. Lichtenberg and M.A. Lieberman, *Regular and Chaotic Dynamics* (Springer, Berlin, 1992).
[11] In Cartesian coordinates $\mathbf{r}=(1.557,-0.236,0.564)$ and $\mathbf{v}=(0.459,-0.267,-0.317)$. The dynamical time $t_D=2\pi|\mathbf{r}|/|\mathbf{v}|\approx 17.0$.
[12] See Eq. (7.7) in H.E. Kandrup, Phys. Rep. **63**, 1 (1980).
[13] C. Siopis and H.E. Kandrup, Mon. Not. R. Astron. Soc. **319**, 43 (2000).
[14] H.E. Kandrup, B.L. Eckstein, and B.O. Bradley, Astron. Astrophys. **320**, 65 (1997), which discusses the pros and cons of the admittedly somewhat simplistic probes of ''complexity'' used in this paper.
[15] K.P. Rauch and S. Tremaine, New Astron. **1**, 149 (1996).
[16] A numerical investigation of the *N*-body problem in the presence of a much larger central point mass [H. Smith, H.E. Kandrup, M.E. Mahon, and C. Siopis, in *Ergodic Concepts in Stellar Dynamics*, edited by V.G. Gurzadyan and D. Pfenniger, Springer Lectures Notes in Physics No. 430 (Springer, New York, 1994), p. 158] suggests that, even if the central mass M_{BH} is much larger than the total mass $M=Nm$ of the individual particles, the *N*-particle orbits continue to exhibit a sensitive dependence on initial conditions. For example, for orbits in simulations with $M_{BH}=10M$, the characteristic time scale t_* associated with the exponential sensitivity was found to be less than three times longer than the value of t_* for $M_{BH}=0$.
[17] Many astrophysicists, including the first author of this paper, had predicted erroneously [*cf.* H.E. Kandrup, Ann. N.Y. Acad. Sci. **848**, 28 (1998)] that the divergence would in fact prove exponential.
[18] More precisely, $\mathbf{r}=(1.557,-0.236,0.564)$ and $\mathbf{v}=(0,0,0)$. The dynamical time $t_D\approx 7.0$.
[19] S. Chandrasekhar, Rev. Mod. Phys. **15**, 1 (1943).
[20] I.V. Pogorelov and H.E. Kandrup, Phys. Rev. E **60**, 1567 (1999).
[21] H.E. Kandrup, R.A. Abernathy, and B.O. Bradley, Phys. Rev. E **51**, 5287 (1995).
[22] M. Tabor, *Chaos and Integrability in Nonlinear Dynamics* (Wiley, New York, 1989).
[23] Recently, as part of his Ph.D. dissertation [I.V. Pogorelov, Ph.D. University of Florida, dissertation, 2001], Pogorelov has made this heuristic argument more convincing. Starting with an exact formula for the second derivative stability matrix $\Phi_{ij}=\partial^2\Phi_N/\partial x^i\partial x^j$ associated with the frozen-*N* potential Φ_N, he derived a formal multidimensional integral expression for the probability distribution $\mathcal{P}(\Lambda)$ for different values of the largest eigenvalue Λ associated with Φ_{ij}, assuming that Φ_N is given as a random sampling of some specified smooth potential Φ. He then proved rigorously that, for certain special cases and geometries, e.g., a test particle located at the center of a constant density system, the largest eigenvalue, which satisfies $\ddot{\delta r}=\Lambda\,\delta r$, is bounded from below by a positive *N*-independent constant; and by implementing a Monte Carlo algorithm to estimate the multidimensional integral, found numerically that Λ appears, if anything, to be a very slowly *increasing* function of *N*. These results do not constitute a rigorous proof that χ remains bounded away from zero — as stressed, e.g., by L. Casetti, C. Clementi, and M. Pettini, Phys. Rev. E **54**, 5969 (1996), χ depends on both the moments of $\mathcal{P}$ and how these moments change in time — but it is almost impossible to envision a setting where the mean value of the largest eigenvalue remains positive but $\chi\to 0$.
[24] Here, $\mathbf{r}=(1.557,-0.236,0.564)$ and $\mathbf{v}=(0.258,-0.267,-0.217)$. The dynamical time $t_D=2\pi|\mathbf{r}|/|\mathbf{v}|\approx 24.0$.